

# Retardation-induced plasmon resonances in coupled nanoparticles

Jörg P. Kottmann and Olivier J. F. Martin

*Electromagnetic Fields and Microwave Electronics Laboratory, Swiss Federal Institute of Technology, ETH-Zentrum, Gloriastrasse 35, 8092 Zurich, Switzerland*

Received January 25, 2001

We study the coupling induced by retardation effects when two plasmon-resonant nanoparticles are interacting. This coupling leads to an additional resonance, the strength of which depends on a subtle balance between particle separation and size. The scattering cross section and the near field associated with this coupled resonance are studied for cylindrical particles in air and in water. Implications for surface-enhanced Raman scattering and nano-optics are discussed. © 2001 Optical Society of America

OCIS codes: 240.6680, 240.5420, 290.5860, 230.1150, 260.3910, 350.3950.

It is a well-known phenomenon that small individual metallic particles of specific metals, such as gold and silver, can support plasmon resonances in the optical wavelength range.<sup>1,2</sup> These plasmon resonances play an important role in, for example, surface-enhanced Raman scattering (SERS), where the Raman signal of molecules adsorbed on these particles is enhanced by the strong near field associated with the plasmon resonances.<sup>3,4</sup>

When two plasmon-resonant nanoparticles are brought together, the plasmon modes in the individual particles can interact, leading to additional resonances for the coupled system.<sup>5-7</sup> These resonances have been investigated in detail when the external field  $\mathbf{E}^0$  is such that both particles are driven in phase. In this Letter we study another coupling mechanism that can occur when the particles are driven out of phase. The resulting resonance is therefore induced solely by the phase advance, or retardation, as light propagates with a finite speed through the particles.

All the results presented in this Letter were obtained with a newly developed technique for scattering calculations, based on the solution of the electric field integral equation by use of finite elements. We refer the reader to Ref. 8, in which this technique is described in detail and its convergence and suitability for computing the plasmon resonances in arbitrarily shaped scatterers are also assessed.

The geometry is depicted in Fig. 1. Two cylinders with the same diameter  $d$  and a separation distance  $a$  are illuminated with a plane wave propagating in the  $\mathbf{k}$  direction, with the electric field  $\mathbf{E}^0$  polarized in the same plane (so-called TE polarization; no plasmon resonances can be excited for the other polarization when the electric field is normal to the figure). Two different incident polarizations  $\mathbf{E}^0$  are investigated. Throughout this Letter we consider silver cylinders and use the experimental data from Johnson and Christy<sup>9</sup> for the permittivity,  $\epsilon(\lambda)$ , as a function of the wavelength,  $\lambda$ .

In Fig. 2 we show the scattering cross section (SCS) for cylinders of various diameters  $d$ . The spacing  $a$  is scaled proportionally so that the ratio  $d/a$  remains constant:  $d/a = 5$ . Figure 2(a) shows the SCS when the

incident electric field  $\mathbf{E}^0$  is parallel to the line joining the cylinders' centers ( $\mathbf{E}^0 \parallel \mathbf{e}_x$ , Fig. 1). One can recognize two resonances in the figure. The first one, near  $\lambda = 340$  nm, corresponds to the resonance of an isolated silver cylinder.

The second resonance visible in Fig. 2(a) results from the interaction of the two cylinders. It is associated with polarization charges, corresponding to the divergence of the electric field, that oscillate in phase on both cylinders, as illustrated in Fig. 1(a). Note that the distribution illustrated in Fig. 1(a) corresponds to an arbitrary snapshot: during one period, the polarization charges oscillate so that, after half a period, the same distribution but with opposite sign is observed, as illustrated in the movies in Ref. 10 for the case of irregularly shaped individual particles.

The coupling between the cylinders influences the corresponding charge distribution: The charge density is more concentrated on the sides of the gap between the particles than on the external sides [Fig. 1(a)]. Therefore the only requirement for this

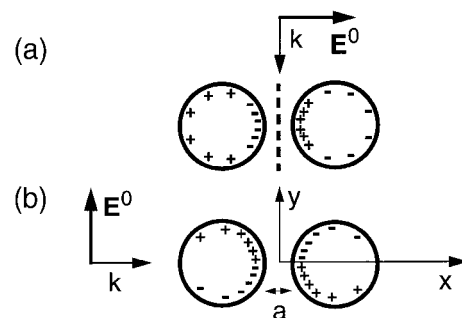


Fig. 1. Two silver cylinders with the same diameter  $d$  and a separation distance  $a$  are illuminated with a plane wave propagating in the  $\mathbf{k}$  direction with incident electric field  $\mathbf{E}^0$ . The distributions of the positive and negative polarization charges corresponding to the two coupled modes visible in Fig. 2 are also shown: (a) When the external field  $\mathbf{E}^0$  is parallel to the line joining the particles, the charges oscillate in phase and the positive and negative charges accumulate on the sides of the gap. (b) For the other illumination direction, when the particles are large enough that their driving fields are out of phase, another mode can be excited.

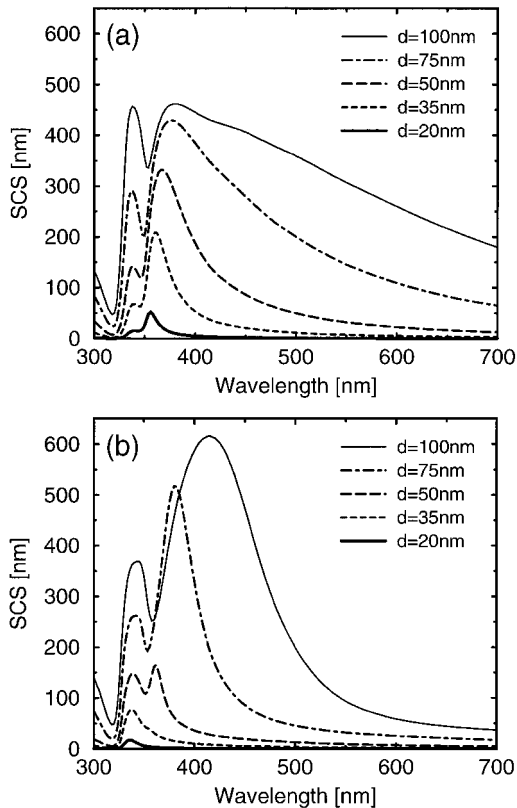


Fig. 2. SCS for two interacting cylinders as a function of the diameter  $d$ . The separation  $a$  is scaled with  $d$ , such that the ratio  $d/a = 5$  remains constant. Two incident polarizations are considered: (a)  $\mathbf{E}^0 \parallel \mathbf{e}_x$  [corresponding to Fig. 1(a)] and (b)  $\mathbf{E}^0 \parallel \mathbf{e}_y$  [Fig. 1(b)].

coupling to occur is that the separation distance  $a$  be small enough. This is the reason why this resonance exists for any particles size, including extremely small ones [Fig. 2(a)].

A very different behavior is observed for the other illumination direction, as illustrated in Fig. 2(b). For small particles, only the resonance around  $\lambda = 340$  nm associated with the individual cylinder is visible. It is only when the particles reach a diameter of  $\sim 50$  nm that a second mode starts to appear [Fig. 2(b)].

The polarization-charge distribution associated with this second mode is illustrated in Fig. 1(b). In this resonance the electric field driving each scatterer is out of phase. This mode is therefore induced solely by the phase advance, or retardation, as the incident field propagates through the structure. The mode is the result of a subtle balance between particle size and separation: Small separation is required for the coupling between the particles, which in turn requires large enough scatterers that their driving fields are out of phase. Note that in Fig. 2, as expected, all the resonances broaden as the size of the cylinders increases.<sup>11</sup>

To illustrate the role played by retardation, we show in Fig. 3 the SCS for the same geometry as in Fig. 2 but with a water background ( $\epsilon_w = 1.78$ ).<sup>12</sup> As anticipated, the overall SCS is more complex, with more resonances than in the vacuum case [compare Figs. 2(b) and 3]. One can see that the dimension onset  $d$  where

the retardation-induced resonance appears is now reduced. This is simply caused by the shorter wavelength in the surrounding medium, so that the required phase difference between both scatterers already occurs for particles of the order of  $d \approx 35$  nm.

The SCS indicates the amount of light scattered in the far field. The field distribution at the vicinity of the particles is also very important. It plays, for example, a crucial role in SERS,<sup>3,4</sup> near-field optics,<sup>13</sup> and nonradiative optical transfer.<sup>14,15</sup> In Fig. 4 we show the near-field distribution between the particles along the dashed line indicated in Fig. 1(a). The same geometries as in Fig. 2 are considered. The cylinders are illuminated with a unit-amplitude plane wave. The amplitudes shown in Fig. 4 give the enhancement caused by the cylinders. The field distributions are computed for the wavelength corresponding to the maximum SCS, so a different wavelength is used for each cylinder's dimensions.

We observe very different behavior depending on the illumination direction. For the incident field along the illumination axis, the field in the gap is strongly enhanced for very small particles. For  $d = 20$  nm, the field amplitude reaches 24 times that of the illumination field [Fig. 4(a)]. This corresponds to an intensity enhancement of more than 500 or a SERS enhancement of more than  $3 \times 10^5$  (SERS enhancement is proportional to the fourth power of the amplitude enhancement<sup>4</sup>).

For larger particles, the field in the gap decreases [Fig. 4(a)]. This result could actually be expected from the SCS in Fig. 2(a): Although the maximum SCS increases for larger particles, the corresponding resonance broadens immensely, indicative of a weaker near field.<sup>11</sup>

For the other illumination direction, since the field is now computed along a line normal to the propagation direction, a symmetrical field distribution is observed [Fig. 4(b)]. The amplitude distribution is perfectly symmetrical, with a minimum in the gap and two maxima on each side of the horizontal axis, which can be related to the polarization charges depicted in Fig. 1(b). Note that the field amplitude on just the horizontal axis is not a good signature for this resonance.<sup>16</sup>

For this polarization the field enhancement between the particles reaches a maximum for  $d \approx 50$  nm

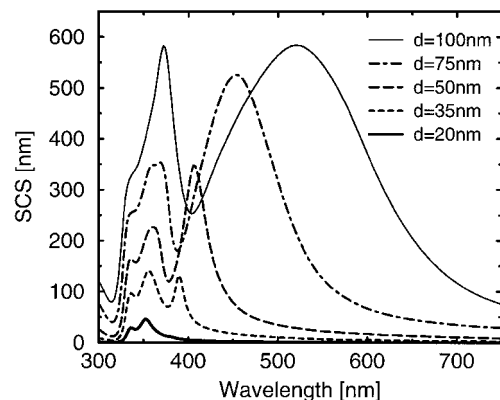


Fig. 3. Same situation as in Fig. 2(b) but with a water background ( $\epsilon_w = 1.78$ ).

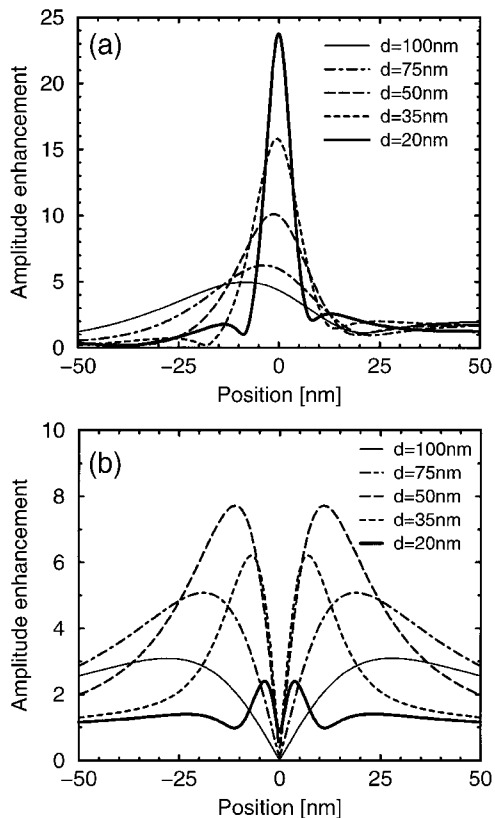


Fig. 4. Amplitude enhancement as a function of the observation position in the gap between the two particles (dashed line in Fig. 1). Same geometry as in Fig. 2. Two incident polarizations are considered: (a)  $\mathbf{E}^0 \parallel \mathbf{e}_x$  [corresponding to Fig. 2(a)] and (b)  $\mathbf{E}^0 \parallel \mathbf{e}_y$  [Fig. 2(b)].

[Fig. 4(b)], which corresponds to the mode onset visible in Fig. 2(b). For a water background, the near-field has already reached a maximum for particles of the order of  $d \approx 35$  nm, which corresponds to the dimensions where this retarded resonance appears in water (see Fig. 3).

These results for interacting particles, together with recent calculations for nonregularly shaped particles,<sup>10,11</sup> should develop our insight into the plasmon resonances in complex systems. They could help us to design specific nanoparticle configurations in which extremely intense and localized electromagnetic fields are established in a controlled manner.

This plasmon-resonance engineering should pave the way toward useful applications in near-field optical imaging,<sup>13</sup> single-molecule detection with SERS,<sup>16–18</sup> and nonradiative optical transport.<sup>14,15</sup> Further, the strong frequency sensitivity of these coupled resonances could be used to produce frequency-selective devices.

We are most indebted to S. Schultz and D. R. Smith, who triggered our interest for plasmon-resonant nanoparticles. This work was supported by the Swiss National Science Foundation. O. J. F. Martin's e-mail address is martin@ifh.ee.ethz.ch.

## References

1. C. F. Bohren and D. R. Huffman, *Absorption and Scattering of Light by Small Particles* (Wiley, New York, 1983).
2. U. Kreibig and M. Vollmer, *Optical Properties of Metal Clusters*, Vol. 25 of Springer Series in Material Science (Springer-Verlag, Berlin, 1995).
3. H. Metiu, *Prog. Surf. Sci.* **17**, 153 (1984).
4. M. Moskovits, *Rev. Mod. Phys.* **57**, 783 (1985).
5. P. K. Aravind, A. Nitzan, and H. Metiu, *Surf. Sci.* **110**, 189 (1981).
6. Y. Xu, *Appl. Opt.* **34**, 4573 (1995).
7. M. I. Mischenko, D. W. Mackowski, and L. D. Travis, *Appl. Opt.* **21**, 4589 (1995).
8. J. P. Kottmann and O. J. F. Martin, *IEEE Trans. Antennas Propag.* **48**, 1719 (2000).
9. P. B. Johnson and R. W. Christy, *Phys. Rev. B* **6**, 4370 (1972).
10. J. P. Kottmann, O. J. F. Martin, D. R. Smith, and S. Schultz, *New J. Phys.* **2**, 27.1 (2000), <http://njp.org>.
11. J. P. Kottmann, O. J. F. Martin, D. R. Smith, and S. Schultz, *Opt. Express* **6**, 213 (2000), <http://www.opticsexpress.org>.
12. M. Bass, ed., *Handbook of Optics*, 2nd ed. (McGraw-Hill, New York, 1995), Vol. I, Chap. 43.8.
13. J. P. Kottmann, O. J. F. Martin, D. R. Smith, and S. Schultz, *J. Microsc.* **202**, 60 (2001).
14. M. Quinten, A. Leitner, J. R. Krenn, and F. R. Aussenegg, *Opt. Lett.* **23**, 1331 (1998).
15. J.-C. Weeber, A. Dereux, C. Girard, J. R. Krenn, and J.-P. Gouyonnet, *Phys. Rev. B* **60**, 9061 (1999).
16. H. Xu, E. J. Bjerneld, M. Käll, and L. Börjesson, *Phys. Rev. Lett.* **83**, 4357 (1999).
17. K. Kneipp, Y. Wang, H. Kneipp, L. T. Perelman, I. Itzkan, R. R. Dasari, and M. S. Feld, *Phys. Rev. Lett.* **78**, 1667 (1997).
18. S. Nie and S. R. Emory, *Science* **275**, 1102 (1997).